Proceedings of the Canadian Society for Mechanical Engineering International Congress
32nd Annual Conference of the Computational Fluid Dynamics Society of Canada
Canadian Society of Rheology Symposium
CSME/CFDSC/CSR 2025
May 25–28, 2025, Montréal, Québec, Canada

Haptic Robotic Hand Design and Control with Neural-Network Based System Identification

Nuo Chen, Ya-Jun Pan*

Department of Mechanical Engineering, Dalhousie University, Halifax, Canada, B3H 4R2
*yajun.pan@dal.ca

***Abstract*—**In this paper, the detailed design of a new and low-cost robotic hand with integrated force sensors for fingertip force control is presented. Compared with other grippers, our gripper can achieve low-cost force tracking by incorporating low-cost motors and force sensors while utilizing a neural network to identify the motors' nonlinear model. Data from the motors and force sensors are processed and communicated using the Robot Operating System (ROS). A proportional–integral–derivative (PID) controller ensures force tracking. The haptic robotic hand is going to be integrated with robotic manipulator for future human-robot interaction and dexterous grasping tasks through human demonstrations.

***Keywords-component*—Gripper; Force; Neural Network; Identification**

I. Introduction

In recent years, there has been a surge in the use of robotic manipulators and humanoid robots in industry. Robots are seen in a wide range of industries and are used in many different applications, from picking up and placing objects in home-life scenarios to moving goods in large factories. With the development of deep learning and the improvement of computational simulation capabilities, position-based control algorithms have developed rapidly as positions are more readily available in simulation environments as well as in human demonstrations. He et al. proposed a learning-based full-body humanoid remote control and autonomy system. The remote control is operated through a virtual reality headset, verbal commands, and a camera to collect information so that humanoid robots can do whole-body tasks through teleoperation or autonomy, such as playing multiple sports, moving and manipulating objects [1]. In [2], Chen et al. demonstrated multiple times to make the learning trajectory smooth so that the manipulator can learn from the human arm and hand position trajectories to do pick-and-place tasks.

Current manipulator end-effectors are basically two-degree-of-freedom (2-DOF) grippers. To achieve more precise operation, both manipulator and humanoid robots need an end-effector with a higher DOF. In [3], Shaw et al. proposed LEAP Hand, which is suitable for machine learning research. It can perform several manipulation tasks in the real world by using teleoperation and learning from videos. Tang et al. used Shadow Hand to possess the skills of manipulating hand tools like dealing with the chain of contacts [4]. Makino et al. developed a five-finger robotic hand that combines machined springs and variable stiffness joints to achieve a wide range of motion for the thumb and adduction and abduction functions for the four fingers [5]. The design allows the manipulator to grasp a variety of objects and exert a large gripping force. Li et al. developed Tactile SoftHand-A, which is three-dimensional (3D) printed, highly underdriven, and requires only two actuators to perform complex grasping maneuvers [6]. Its unique dual-tendon design allows active control of specific joints to adjust the gripping posture of the hand.

Although the aforementioned multi-DOF grippers can accomplish more tasks, they are expensive, especially for the force sensors. In this paper, we designed a three-finger robotic hand, which has the advantage of being simple and inexpensive, while enabling flexible gripping and manipulation of a wide range of objects. The three-finger design mimics the dexterity of human fingers and is able to handle objects of different shapes and sizes, improving the adaptability and flexibility of the robotic hand. However, there are still many challenges in realizing the robotic finger tip force control. In particular, movements that mimic human finger tip forces require precise sensing and control systems when the hand mimics these movements [7].

The position control of grippers is the basic research di-

This work was supported by the Natural Sciences and Engineering Research Council (NSERC) and the Government of Nova Scotia, Canada.

rection for all types of grippers because, like robot position control, hand position information is more intuitive and easier to obtain by encoders and cameras in simulation environments as well as in human demonstrations. In [8], Palleschi developed an algorithm that generates candidate grasps by breaking objects down into fundamental shapes, enabling the approach to adapt to various object geometries. The demonstrations are generated by human motion. Not coincidentally, Chen et al. also used a camera to capture human demonstrations and generate the end position of the manipulator as well as the opening and closing movements of the gripper [9].

However, a position control cannot accomplish all tasks for grippers. For more delicate tasks, such as wiping a table with different forces and squeezing deformable objects, a position control only cannot accomplish these tasks. In [10], Gunderman et al. presented a tendon-driven soft gripper with contact force feedback control. This gripper leverages passive compliance to allow the gentle harvesting of berries by applying a preset force by each finger. Yu et al. [11] proposed a neural network-based adaptive force tracking control of a flexible articulator, which realizes high-precision control under uncertainty conditions by dynamically adjusting the control parameters online. This method can show a good pressure force control effect in the table wiping task.

Although the above literature have done some research on gripper force control, there are still several problems with force control of robotic grippers: 1) Grippers that can realize force control are too expensive, for example, Shadow hands cost €25K to €200K [12], which hinders the development of robots. The price of fine force sensors is too high so grippers are expensive. 2) The output of the force sensors is quite noisy, which is also the main obstacle of the force control of the robotic gripper.

Therefore, we designed a low-cost gripper that includes a force sensor on every finger. This gripper has three fingers and three motors for each finger to ensure 3D position accessibility. Each finger has a low-cost force sensor that can be used for system identification of the motors and real-time force control. A neural network is applied to generate a nonlinear model for the motor. All the information of this gripper can be communicated and implemented through the Robot Operating System (ROS).

II. Haptic Robotic Hand Design

In this chapter, the mechanical design and software design of the robotic hand are introduced. The mechanical design includes the design of the kinematics of the gripper and force sensor circuit.

A. Mechanical Design

Referring to the design of the BarrettHand [13], we designed the gripper as three fingers, each with three motors to ensure flexibility of the end joints of the fingers in three dimensions. The motor is XL330-M288-T manufactured by Dynamixel. Its small size and weight of only 18g and its ability to generate up to 0.6Nm of torque make it an ideal motor for the gripper. This motor is also applied in recent work [14]. This kind of modular design is quite convenient for future maintenance and part replacement if there are any failures in the device.

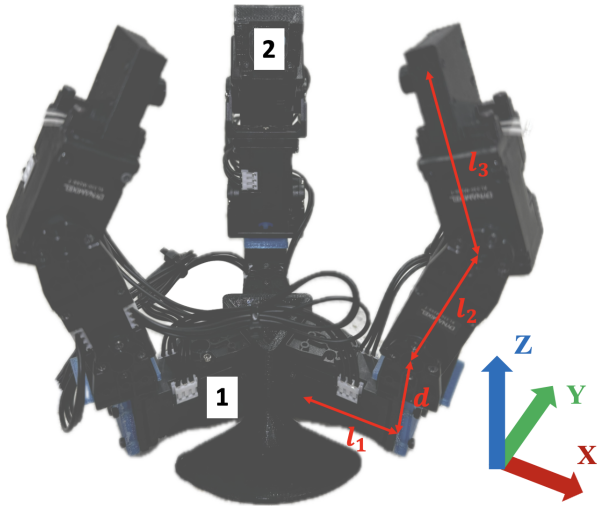

Figure. 1. Mechanical Design. 1) Dynamixel XL330-M288-T motor, 2) Flexiforce A201-25 force sensor.

As shown in Fig. 1, the motor at the bottom of each finger rotates in a vertical direction, while the rotation axis of the other two motors rotates in a horizontal direction. Therefore, the position $\boldsymbol{p}$ of one finger end-effector can be represented by Eq. (1):

$$\boldsymbol{p} = \begin{bmatrix} x \\ y \\ z \end{bmatrix} = \begin{bmatrix} (l_1 + l_2c_2 + l_3c_{23})c_1 \\ (l_1 + l_2c_2 + l_3c_{23})s_1 \\ d + l_2s_2 + l_3s_{23} \end{bmatrix}, \tag{1}$$

where $s_i = sin(q_i), c_i = cos(q_i), s_{ij} = sin(q_i + q_j), c_{ij} = cos(q_i + q_j)$, l_i represents the ith link length, and d represents the displacement between motor 1 and 2.

To generate the torque of each motor with a given force, the Jacobian matrix is needed. The Jacobian matrix of this gripper is shown in Eq. (2).

$$J(\boldsymbol{q}) = \begin{bmatrix} -rs_1 & -l_2s_2c_1 - l_3s_{23}c_1 & -l_3c_1s_{23} \\ rc_1 & -l_2s_2s_1 - l_3s_{23}s_1 & -l_3s_1s_{23} \\ 0 & l_2c_2 + l_3c_{23} & l_3c_{23} \end{bmatrix}, \tag{2}$$

where $r = l_1 + l_2c_2 + l_3c_{23}$. With the Jacobian matrix, the torque $\boldsymbol{\tau}$ of each joint given by finger end-effector force $\boldsymbol{F}$ can be generated by:

$$\boldsymbol{\tau} = J(\boldsymbol{q})^T \boldsymbol{F}. \tag{3}$$

To apply a human hand force demonstration to a robotic gripper, a force sensor device is required. Each finger of the gripper has a similar sensor setup at the tip of the finger to obtain the pressure at the end of the gripper in real time. The force sensor is a low-cost piezoresistor that outputs different voltage signals in a circuit depending on the amount of pressure. The circuit diagram as shown in Fig. 2 includes an amplifier, resistor, and capacitor to reduce the force sensor

signal noise. The amplifier model is MCP6004, the resistor R is 100K Ω and the capacitor C is 47 pF. We utilized Arduino UNO to capture the voltage signal and used two batteries to provide positive 5V and -5V voltage respectively.

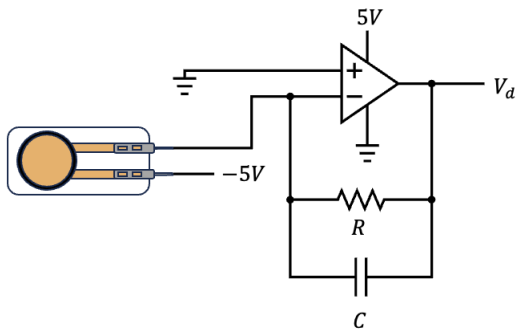

Figure. 2. Force Sensor Circuit.

B. Software Design

As illustrated in Fig. 3, the gripper force sensor output is collected by an Arduino UNO board which sends data to the laptop through ROS and package rosserial_python in real-time. The gripper motor is actuated by the python module of Dynamixel_SDK in the Ubuntu system and uses current-based position control mode with reference current and encoder positions. This is ideal for articulated robots and grippers. The communication between the laptop and the Dynamixel motor was accomplished through a U2D2 converter and U2D2 power hub board. Although many Dynamixel motors use the OpenRB-150 as the driver board, OpenRB-150 does not communicate well in ROS.

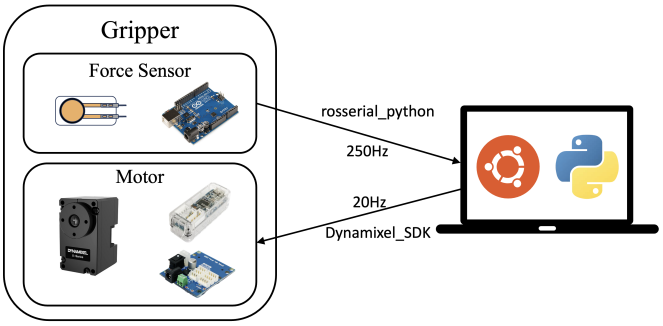

Figure. 3. Communication Framework.

III. Methodology

This section shows the methods to transfer force sensor voltage to real force and new neural-network based system identification.

A. Voltage-Force Conversion

Although the voltage trajectory given by the force sensor represents the trend of the force, it is still not a force in the definition of a physical quantity. Therefore, we need to establish a connection between the force and voltage. We tested the voltage as a function of force by applying different weights of objects to the sensor, and the curve fitted result is shown in Fig. 4. The force sensor has a deadzone of less than 2N and does not return a value.

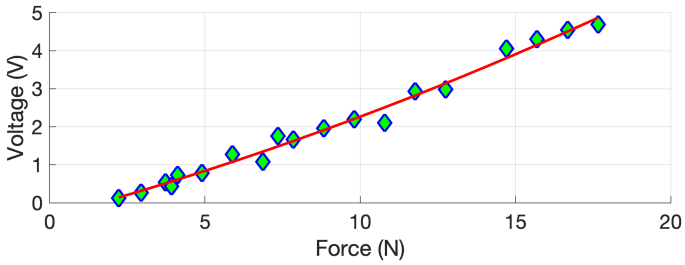

Figure. 4. Voltage-Force Calibration. The green rhombic represents data of different weights and the red curve represents the fitted quadratic function.

The fitting curve we choose is a quadratic function shown in Eq. (4). Since F is a positive number, there is only one solution. According to the data from different weight objects, the parameters of Eq. (4) is $a = 0.0043, b = 0.2207, c = -0.3724$.

$$\begin{aligned} V &= aF^2 + bF + c, \\ F &= \frac{-b + \sqrt{b^2 - 4a(c - V)}}{2a}, \end{aligned} \tag{4}$$

where V is the voltage.

B. Neural Network System Identification

We took Dynamixel XL330-M288-T motors as gripper motors. Since the gripper motor needs to be small, the motor chosen was limited in size, torque could not be measured, and the torque-current function was not provided. The other motor, the XC330-M288-T, offers a torque-current function, but the function is not linear. So we cannot use

$$\tau = KI, \tag{5}$$

as the torque-current function.

A neural network can be applied to identify the system model of the motor, which requires a huge amount of data on the torque and current. Since the torque is not measurable, we developed a device in Fig. 5 to calibrate and test the voltage signal of the force sensor in the fingertip and then transform it to force and torque, respectively.

$$\tau = FL. \tag{6}$$

Using Eq. (4) and Eq. (6) we can convert the voltage signal data to the corresponding torque output. The data collected by this device is shown in Fig. 6. The blue data represents torque values and orange data represents current signals. The blue curves are noisier because these data are collected by force sensors and therefore contain noise. The

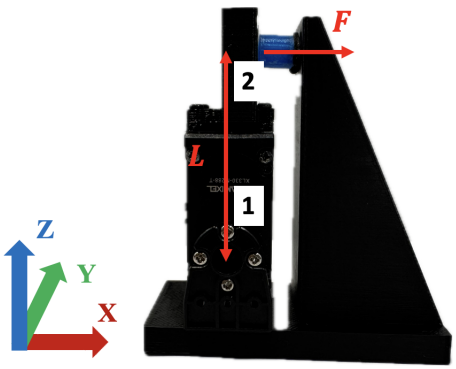

Figure. 5. System Identification Setup. 1) Dynamixel XL330-M288-T motor, 2) Flexiforce A201-25 force sensor.

orange data is smoother because the current signal comes from the motor. The torque values occasionally spikes as the current is generated, indicating that the force sensor can overshoot when the force changes more rapidly. The current signal is obtained according to a function that we set up. A step function is chosen for data acquisition because the value of the force sensor decreases after a period of continuous triggering. Although this feature can be ignored when mimicking the force curve demonstrated by a human because the gripper takes the same amount of time to do the action, for system modeling this feature can lead to an inaccurate model.

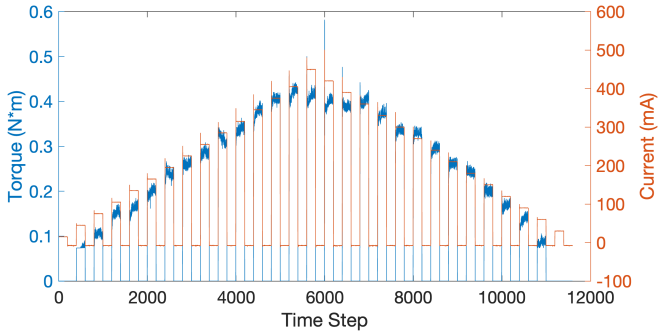

Figure. 6. System Identification Data Collection.

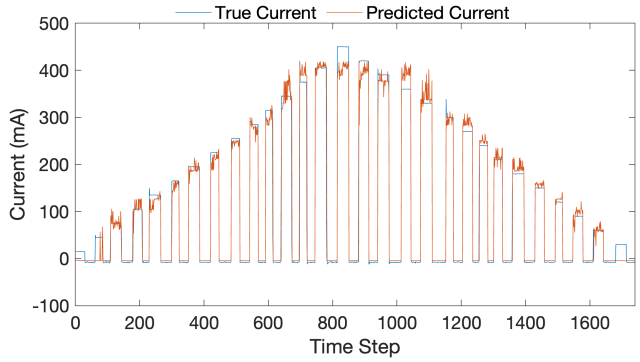

Figure. 7. Neural-Network Prediction.

The neural network we choose is the fully connected neural network. To train the neural network, 70% of the data in Fig. 6 is used as training data, 15% as validation data, and the remaining 15% as test data. The hidden layer of the neural network contains 64 and 32 neurons, and the activation function is a tansig function with a maximum training epoch of 1000 and a learning rate of 0.001. All training data were normalized with the zscore function before training.

The neural network prediction results are shown in Fig. 7. The blue curve is the true current and the orange curve is the current prediction obtained by the trained neural network using the force sensor data as input. It can be seen from the figure that the predicted values are noisy and there are errors from the actual values. The reason for this is that the input data, which is the force sensor data, is noisy and hence the output produced by the network is also noisy. Hence in the future work, the neural network structure needs to be refined to minimize the noise from the input signal.

IV. Experiment

The block diagram of the experiment is shown in Fig. 8. The demonstrated force data from the human and the end-effector force data provided by the robotic hand are transferred to the desired voltage $\boldsymbol{V_d}$ and actual voltage $\boldsymbol{V_r}$ through the sensor circuit shown in Fig. 2. The voltage-force conversion converts the voltage $\boldsymbol{V}$ to force $\boldsymbol{F}$ by Eq. (4). The reference force trajectory $\boldsymbol{F_d}$ can be converted to a torque trajectory $\boldsymbol{\tau_d}$ for each motor based on inverse kinematics, and then converted to a reference current $\boldsymbol{I_d}$ for each motor by a trained neural network. The controller generates the current $\boldsymbol{I}$ as the input for the motors based on the error force $\boldsymbol{F_e}$ and the reference current $\boldsymbol{I_d}$. The controller we use in the experiment is a proportional–integral–derivative (PID) controller as shown in Eq. (7),

$$\boldsymbol{I} = \boldsymbol{I_d} + K_p \boldsymbol{F_e} + K_i \int \boldsymbol{F_e}(t)dt + K_d \frac{d\boldsymbol{F_e}}{dt}, \qquad (7)$$

with parameters $K_p = 40, K_i = 1$, and $K_d = 1$.

In order to verify the effectiveness of the experimental framework, the robotic hand is asked to achieve force tracking by squeezing a bottle with a fixed gesture. The motor position of each finger is the same, the angle of the motor located at the bottom q_1 is 0 degrees, the angle of the motor located at the center q_2 is 120 degrees, and the angle of the motor located at the top q_3 is -30 degrees. Two experiments with reference force magnitudes of 3.6N and 4N in x-axis are carried out, and the experimental results are shown in Fig. 9 and Fig. 10. Two experiments with different desired forces are set up to verify the tracking effect of the controller for different desired forces with the same parameters.

As shown in Fig. 9 and Fig. 10, the robotic hand can realize the tracking of different forces in 2 seconds. However, due to the error of the sensor and the noise, the force applied by the gripper is always changing and not smooth enough. In general, the force tracking is not perfect but with small acceptable errors.

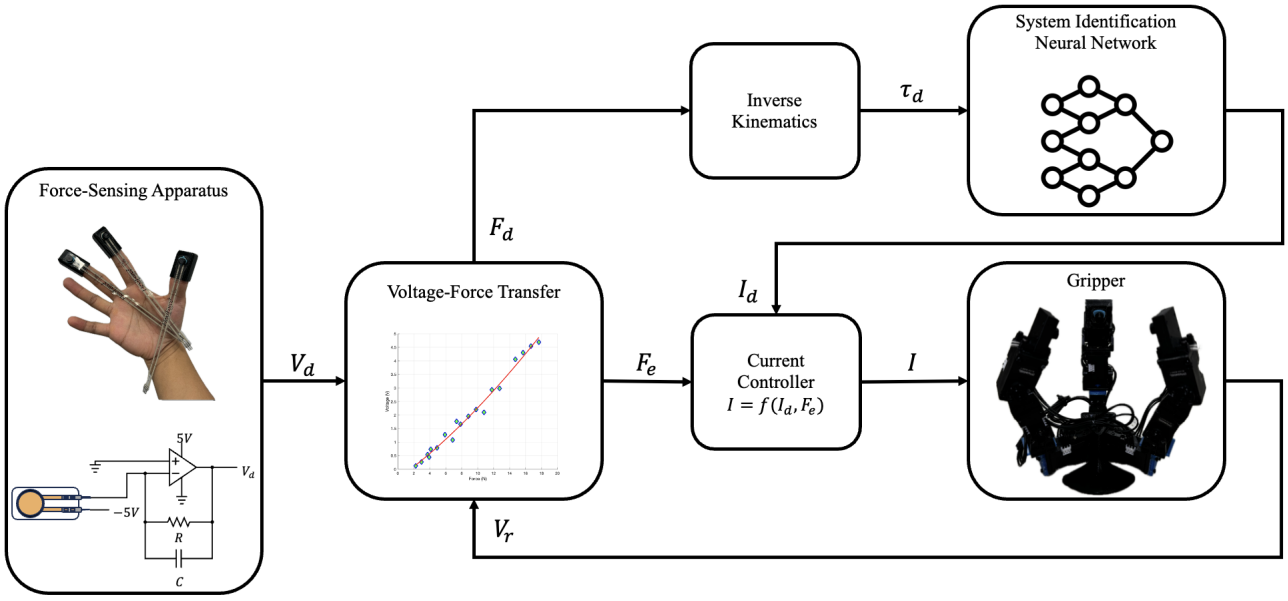

Figure. 8. Schematic Diagram of the Experiment.

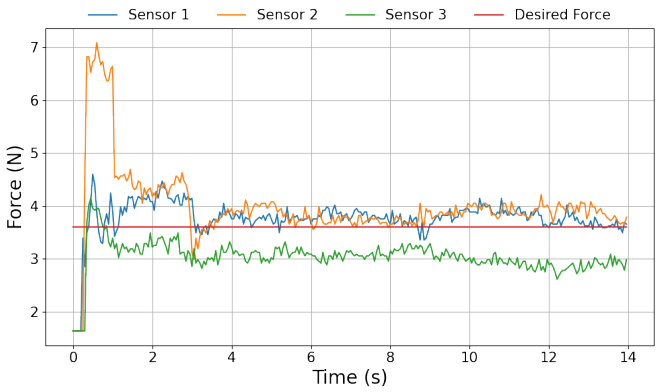

Figure. 9. Force Tracking of a Reference 3.6N.

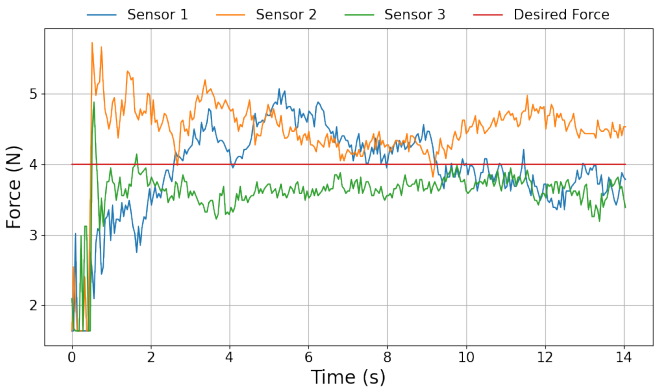

Figure. 10. Force Tracking of a Reference 4N.

V. Conclusion and Future Work

In this paper, we build a low-cost haptic robotic hand. Through the kinematic analysis of the gripper, the design of the force sensor circuit, the communication between different components in the ROS framework, and the modeling of the motor by the neural network, we built an experimental framework for force tracking using the device. Two experiments demonstrated that the robotic hand can realize force following with a good performance.

The limitation of this work is that the force control is not precise enough. Currently, the force tracking and motor modeling is limited by sensor noise and errors that prevent accurate control, so it is expected that sensor errors can be captured and compensated by neural networks and other control methods can be applied in the future to allow the gripper to achieve more accurate force tracking. The device will be integrated to the Franka Emika Panda robotic manipulator in the Advanced Control and Mechatronics Lab in the future for dexterous manipulation.

Acknowledgment

The authors would like to thank Juliette Palfray, Barrett Sapunjis, Jack Xue, and Kaichen Zhou for the construction of the robotic hand prototype.

References

[1] T. He, Z. Luo, X. He, W. Xiao, C. Zhang, W. Zhang, and G. Shi, "OmniH2O: Universal and dexterous human-to-humanoid whole-body teleoperation and learning," arXiv preprint arXiv:2406.08858, 2024.

[2] N. Chen, L. Wan and Y. -J. Pan, "Robust and Adaptive Dexterous Manipulation With Vision-Based Learning From Multiple Demonstrations," in IEEE Transactions on Industrial Electronics, In Press, 2024.

[3] K. Shaw, A. Agarwal, and D. Pathak, "LEAP Hand: Low-Cost, Efficient, and Anthropomorphic Hand for Robot Learning," in Robotics: Science and Systems (RSS), 2023.
[4] L. Tang, Y. -B. Jia and Y. Xue, "Robotic Manipulation of Hand Tools: The Case of Screwdriving," 2024 IEEE International Conference on Robotics and Automation (ICRA), Yokohama, Japan, 2024, pp. 13883-13890.
[5] S. Makino et al., "Five-Fingered Hand with Wide Range of Thumb Using Combination of Machined Springs and Variable Stiffness Joints," 2018 IEEE/RSJ International Conference on Intelligent Robots and Systems (IROS), Madrid, Spain, 2018, pp. 4562-4567.
[6] H. Li, C. J. Ford, C. Lu, et al., "Tactile SoftHand-A: 3D-printed, tactile, highly-underactuated, anthropomorphic robot hand with an antagonistic tendon mechanism," arXiv preprint arXiv:2406.12731, 2024.
[7] Tasi, B. J., Koller, M., and Cserey, G., "Design of the anatomically correct, biomechatronic hand," arXiv preprint arXiv:1909.07966, 2019.
[8] A. Palleschi et al., "Grasp It Like a Pro 2.0: A Data-Driven Approach Exploiting Basic Shape Decomposition and Human Data for Grasping Unknown Objects," in IEEE Transactions on Robotics, vol. 39, no. 5, pp. 4016-4036, Oct. 2023.
[9] N. Chen and Y. -J. Pan, "Vision-Based Dexterous Motion Planning by Dynamic Movement Primitives with Human Hand Demonstration," 2024 IEEE 33rd International Symposium on Industrial Electronics (ISIE), Ulsan, Korea, Republic of, 2024, pp. 1-6.
[10] A. L. Gunderman, J. A. Collins, A. L. Myers, R. T. Threlfall and Y. Chen, "Tendon-Driven Soft Robotic Gripper for Blackberry Harvesting," in IEEE Robotics and Automation Letters, vol. 7, no. 2, pp. 2652-2659, April 2022.
[11] X. Yu, S. Liu, S. Zhang, W. He and H. Huang, "Adaptive Neural Network Force Tracking Control of Flexible Joint Robot With an Uncertain Environment," in IEEE Transactions on Industrial Electronics, vol. 71, no. 6, pp. 5941-5949, June 2024.
[12] Shadow Robot, "How much does a robot hand cost?" Shadow Robot Blog, [Online]. Available: https://www.shadowrobot.com/blog/how-much-does-a-robot-hand-cost/.
[13] G. Rauso, R. Caccavale and A. Finzi, "Incremental Learning of Robotic Manipulation Tasks through Virtual Reality Demonstrations," 2024 IEEE/RSJ International Conference on Intelligent Robots and Systems (IROS), Abu Dhabi, United Arab Emirates, 2024, pp. 5176-5181.
[14] Z. Yun et al., "A Study of Lightweight, Low-cost Quadrupedal Robot Body Based on a Coaxial Deformation Mechanism," 2024 IEEE International Conference on Mechatronics and Automation (ICMA), Tianjin, China, 2024, pp. 1320-1325.